International Journal of Chemical Engineering Research.
ISSN 0975-6442 Volume 9, Number 1 (2017), pp. 7-39

http://www.ripublication.com

Large Eddy Simulation Turbulence Modeling for wind Flow over Wall Mounted Cube

Bibhab Kumar Lodh[1], Ajoy K Das[2] and N. Singh[3]

1(Department of Chemical Engineering, National Institute of Technology Agartala, West Tripura-799046), India.

2 (Department of Mechanical Engineering, National Institute of Technology Agartala, West Tripura-799046), India.

3(Department of Aerospace Engineering, IIT Kharagpur, West Bengal), India.

Abstract

This paper will present the homogeneous dynamic Smagorinsky large eddy simulation of transient turbulence flow for wind flow over a wall mounted 3D cubical model. The domain for this study is of the size of 60 cm x 30 cm x 30 cm. The 3D cube model is taken of the size of 4cm x 4 cm x 4 cm. The Reynolds number for the flow in respect of the height of the cube i.e, 4 cm is 53000. The hexahedral grids are used for the meshing of the flow domain. The results are discussed in terms of various parameters such as velocity profile around the cube and the computational domain, the pressure distribution over the cube, and also the result of drag coefficient is verified by neural network time series analysis using MATLAB. In this present study we have used the OpenFoam platform for the computational and numerical analysis. The numerical scheme employed is the PISO algorithm with the use of LES Homogeneous Dynamic Smagorinsky model. The Fast Fourier transformation of the lift coefficient has been employed to find the highest frequency of the vortex shedding so that the strouhal number can be found. It is observed that there is a constant positive drag coefficient in the later part of the simulation run and a low constant lift coefficient since the design of cube is not aerodynamic. The yplus LES value is also calculated and found as less than unity which is acceptable range for LES turbulence model while in the initial range of the upstream the y plus value is more than unity, because of the coarse mesh in that section due to limitation of computer memory.

Keywords: Large eddy simulation, Smagorinsky, 3D cubical model, PISO algorithm, Reynolds no., OpenFoam, Artificial neural network, MATLAB.

I. INTRODUCTION

Unsteady transient flows around a cube are very significant for many engineering problems. Large Eddy Simulation (LES) of three dimensional flow field around a wall mounted cube with sharp corners is performed numerically which is supposed to be a benchmark problem in turbulence modelling for flow over bluff bodies. The aim of the present work is to find the various parameters like pressure profile, velocity profile, drag and lift forces in time domain around three dimensional flow fields. Turbulent flows are of utmost importance in case of wind flow around bluff bodies such as building, towers etc and are highly influenced by the solid walls around the body. The viscous affected regions are generally governed by the walls and have very large gradients and hence these regions should have accurate presentation for the true prediction of wall bounded flow [1]. Turbulence is an unpredictable state of fluid and is one of the most challenging problems in fluid dynamics. Turbulent flows brings eddies or whirls which ranges from very large scale to very small scale in sizes. Energy is transferred between these scales are generally from larger to smaller scales until finally the smallest scales are dissipated into heat by molecular viscosity. This energy cascade theory was introduced into physical laws for the various scales present in turbulent flow by Russian Scientist Kolmogorov [2]. The study of turbulent flows can be divided in three main categories: Analytical, physical experiments and numerical simulation. Numerical simulation has become very popular in the last couple of decades since it is lot more flexible and cost effective than the real experimental method. Also due to the complexity of the flow behaviour it is not always possible to perform or visualize the experimental results due to lack of high precision equipment or due to the cost of those equipments. Computational methods have been applied in wind engineering to study wind flow pattern around buildings or a group of buildings with a view to understand flow interference effects and its relation to pollution dispersion, pedestrian comfort, ventilation in the building etc. The main complications of using numerical method arise due to bluff body shape of the structures with sharp corners. This configuration has attracted increasing attention from researchers and has been used for the bench-marking purposes to validate turbulent model with numerical methods.Complicated flow fields around buildings consisting of impingement, flow separation, streamline curvature, reattachment and vortex formation remains the most challenging problem to tackle. Further complications arise due to presence of turbulence.

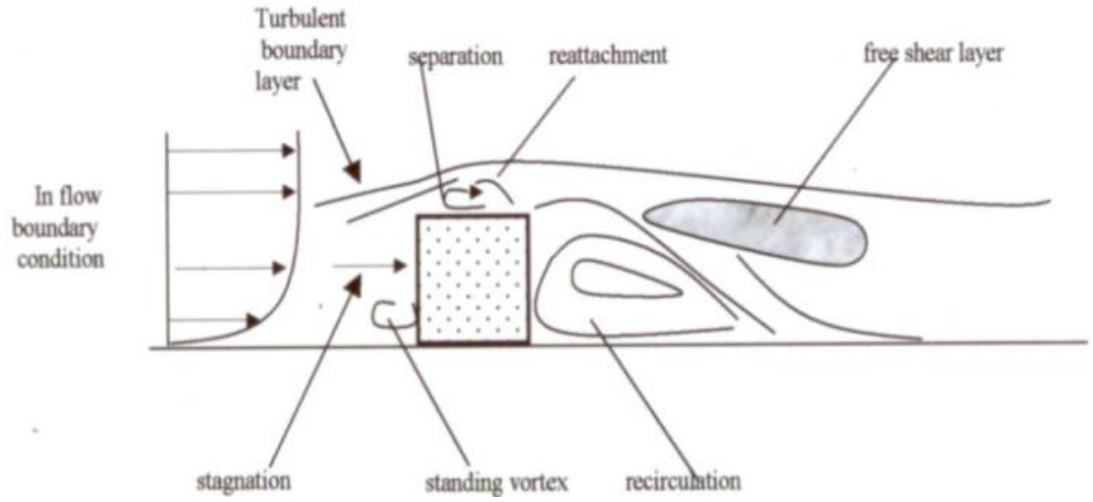

Fig. 1 Typical turbulent flow behaviour over a cubical body

Many experimental works are performed on flow around ground-mounted cube in a developed turbulent channel flow. Results showed that this flow is characterised by the looks of the horseshoe-type vortex at the windward face, associate arc-shaped vortex within the wake of the cube, flow separation at the highest and facet face of the cube and vortex shedding. The flow options and experimental information for time-averaged flow quantities are well documented in Martinuzzi and Tropea [3] and Hussein and Martinuzzi [4]. Experimental study was additionally performed by Meinders' et al. [5] in a very developing turbulent channel flow. The computational method has the advantage over the experimental work that any flow physical quantity can be measured at any point in the flow field and at any instance. One major drawback for the numerical simulation in case of engineering field is that the inability to give accurate result under any given condition and hence it is of utmost importance to validate the result of the simulation. The simulation of turbulent flow or the turbulence modelling has different approach and they can be illustrated as below: The Reynolds Average Navier-Stokes (RANS) is generally used Applications that only require average statistics of the flow. It Integrate merely the ensemble-averaged equations and Parameterize turbulence over the whole eddy spectrum. The advantages of RANS are that it is computationally inexpensive, fast. Whereas the disadvantages are in this turbulent fluctuation not explicitly captured and also pparameterizations are very sensitive to large-eddy structure that depends on environmental conditions such as geometry and stratification Parameterizations are not valid for a wide range of different flows and hence it is not suitable for detailed turbulence studies. Direct Numerical Simulation (DNS) is the most straight-forward approach. It resolves all scales of turbulent flow explicitly. The advantage is that in principle it gives very

accurate representation of flow field. The disadvantage is that it requires high level of computational resources. Hence DNS is restricted to moderately turbulent flow and highly turbulent flows cannot be simulated because of excessive time consumption and cost. The approach what we have implemented in this present study is the Large Eddy Simulation (LES) because of its advantages over the other two approaches of turbulence modelling. It seems to combine advantages and avoid disadvantages of DNS and RANS by treating large scales and small scales separately, based on Kolmogorov's theory of turbulence. The large eddies are explicitly resolved and the impact of small eddies on the large-scale flow is parameterized. The advantage of this method is that hhighly turbulent flows can be simulated. LES does not resolve the full range of turbulent scales (as DNS does), but it captures a much larger range of scales than the Reynolds average equations. Direct simulation is applied to the large scales, while the small scales are averaged out and their effects are modelled. This approach appears to be Justified because the large eddies contain most of the energy, do most of the transporting of conserved properties and vary most from case to case. In contrast, the smaller eddies are believed to be more universal (largely independent of the boundary conditions) and therefore easier to model. Since the contribution of the small-scale turbulence to the resolved flow field is small, the errors introduce by their modelling should also be small. In addition, the resolved scales carry much more information than the mean flow predicted by the RANS approach. LES is therefore potentially much more accurate than RANS and when compared to DNS, its demand on computer resources is considerably smaller, since the smallest scales need not be resolved. In addition, LES surface time-pressure histories have proven to be ideal for predicting low Mach number aero-acoustic noise sources, an important consideration in automotive design and other fields. Given all these factors, the steady increase in computing resources and the advancing development of the technique, LES promises to take a prominent role in design environments of the near future. From the above comparison it is very much clear that the LES modelling is much more suitable for high turbulence and hence we have implemented the LES subgrid model which is supposed to be one of the most suitable turbulence modelling tools. The details of the subgrid model will be discussed in the Numerical Approach section. Most of the numerical simulation on the turbulent flow over a cube were performed using RANS incorporating various turbulent models [6, 7] and Large eddy simulation (LES) [8,9,10,11,12]. The unsteady flow behaviour which has been performed in the present study is done with the LES methods since LES proved to be good agreement with real time experimental result. Whereas the RANS approach could not produce the complex vortex structure within the near wall vicinity because of the boundary layer development in front of the cube [13].

II THEORY OF LARGE EDDY SIMULATION

Turbulent flows are characterized by eddies with a wide range of length and time scales. The largest eddies are typically comparable in size to the characteristic length of the mean flow. The smallest scales are responsible for the dissipation of turbulence kinetic energy.

It is possible, in theory, to directly resolve the whole spectrum of turbulent scales using an approach known as direct numerical simulation (DNS). No modeling is required in DNS. However, DNS is not feasible for practical engineering problems involving high Reynolds number flows. The cost required for DNS to resolve the entire range of scales is proportional to Re_t^3 where Re_t is the turbulent Reynolds number. Clearly, for high Reynolds numbers, the cost becomes prohibitive. In LES, large eddies are resolved directly, while small eddies are modeled. Large eddy simulation (LES) thus falls between DNS and RANS in terms of the fraction of the resolved scales. The rationale behind LES can be summarized as follows:

- Momentum, mass, energy, and other passive scalars are transported mostly by large eddies.
- Large eddies are more problem-dependent. They are dictated by the geometries and boundary conditions of the flow involved.
- Small eddies are less dependent on the geometry, tend to be more isotropic, and are consequently more universal.
- The chance of finding a universal turbulence model is much higher for small eddies.

Resolving only the large eddies allows one to use much coarser mesh and larger times-step sizes in LES than in DNS. However, LES still requires substantially finer meshes than those typically used for RANS calculations. In addition, LES has to be run for a sufficiently long flow-time to obtain stable statistics of the flow being modeled. As a result, the computational cost involved with LES is normally orders of magnitudes higher than that for steady RANS calculations in terms of memory (RAM) and CPU time. Therefore, high-performance computing (e.g., parallel computing) is a necessity for LES, especially for industrial applications.

A Governing equations for LES: the subgrid-scale turbulence models

1. Filtered Navier-Stokes Equations

The governing equations employed for LES are obtained by filtering the time-dependent Navier-Stokes equations in either Fourier (wave-number) space or configuration (physical) space. The filtering process effectively filters out the eddies whose scales are smaller than the filter width or grid spacing used in the computations. The resulting equations thus govern the dynamics of large eddies.

A filtered variable (denoted by an overbar) is defined by

$$\overline{\phi(x)} = \int_D \phi(x')G(x,x')dx' \tag{1}$$

Where D is the fluid domain and G is the filter function that determines the scale of the resolved eddies

The finite-volume discretization itself implicitly provides the filtering operation:

$$\overline{\phi(x)} = \frac{1}{V}\int_v \phi(x')dx', x' \in v \tag{2}$$

Where V is the volume of a computational cell. The filter function, G(x,x'), implied here is then

$$G(x,x') = \begin{cases} \frac{1}{V}, x' \in v \\ 0, \ x' otherwise \end{cases} \tag{3}$$

Filtering the Navier-Stokes equations, one obtains

$$\frac{\partial \rho}{\partial t} + \frac{\partial}{\partial x_i}(\rho \overline{u_i}) = 0 \tag{4}$$

and

$$\frac{\partial}{\partial t}(\rho \overline{u_i}) + \frac{\partial}{\partial x_j}(\rho \overline{u_i}\,\overline{u_j}) = \frac{\partial}{\partial x_j}(\sigma_{ij}) - \frac{\partial \overline{p}}{\partial x_i} - \frac{\partial \tau_{ij}}{\partial x_j} \tag{5}$$

Where σ_{ij} is the stress tensor due to molecular viscosity defined by

$$\sigma_{ij} \equiv \left[\mu\left(\frac{\partial \overline{u_i}}{\partial x_j} + \frac{\partial \overline{u_j}}{\partial x_i}\right] - \frac{2}{3}\mu \frac{\partial \overline{u_i}}{\partial x_i}\delta_{ij} \right. \tag{6}$$

and τ_{ij} is the subgrid-scale stress defined by

$$\tau_{ij} \equiv \overline{\rho u_i u_j} - \rho \overline{u_i}\,\overline{u_j} \tag{7}$$

2. Subgrid-Scale Models

The subgrid-scale stresses resulting from the filtering operation are unknown, and require modeling. The subgrid-scale turbulence models employ the Boussinesq hypothesis [14] as in the RANS models, computing subgrid-scale turbulent stresses from

$$\tau_{ij} - \frac{1}{3}\tau_{kk}\delta_{ij} = -2\mu_t \overline{S_{ij}} \tag{8}$$

Where μ_t is the subgrid-scale turbulent viscosity. The isotropic part of the subgrid-scale stresses τ_{kk} is not modeled, but added to the filtered static pressure term. $\overline{S_{ij}}$ is the rate-of-strain tensor for the resolved scale defined by

$$\overline{S_{ij}} \equiv \frac{1}{2}\left(\frac{\partial \overline{u_i}}{\partial x_j} + \frac{\partial \overline{u_j}}{\partial x_i} \right) \tag{9}$$

As for incompressible flows, the term involving τ_{kk} can be added to the filtered pressure or simply neglected [15]

There are quite a few model for μ_t such as the Smagorinsky-Lilly model, the dynamic Smagorinsky-Lilly model, the WALE model, and the dynamic kinetic energy subgrid-scale model.

The subgrid-scale turbulent flux of a scalar, ϕ, is modeled using subgrid-scale turbulent Prandtl number by

$$q_j = -\frac{\mu_t}{\sigma_t}\frac{\partial \phi}{\partial x_j} \tag{10}$$

where q_j is the subgrid-scale flux.

2.1 Smagorinsky-Lilly Model

This simple model was first proposed by Smagorinsky [16]. In the Smagorinsky-Lilly model, the eddy-viscosity is modeled by

$$\mu_t = \rho L_s^{\,2} \left|\overline{S}\right| \tag{11}$$

Where L_s is the mixing length for subgrid scales and $\left|\overline{S}\right| \equiv \sqrt{2\overline{S_{ij}}\,\overline{S_{ij}}}$. Where, L_s is computed using

$$L_s = \min(\kappa d, C_s \Delta) \tag{12}$$

Where κ is the von Kármán constant, d is the distance to the closest wall, C_s is the Smagorinsky constant, and Δ is the local grid scale.

Lilly derived a value of 0.17 for C_s for homogeneous isotropic turbulence in the inertial subrange. However, this value was found to cause excessive damping of large-scale fluctuations in the presence of mean shear and in transitional flows as near solid

boundary, and has to be reduced in such regions. In short, C_s is not a universal constant, which is the most serious shortcoming of this simple model. Nonetheless, a C_s value of around 0.1 has been found to yield the best results for a wide range of flows

2.2 Dynamic Smagorinsky-Lilly model

In the dynamic models, the subgrid-scale turbulent Prandtl number or Schmidt number is obtained by applying the dynamic procedure originally proposed by Germano [17] to the subgrid-scale flux. Germano et al. [17] and subsequently Lilly [18] conceived a procedure in which the Smagorinsky model constant, C_s, is dynamically computed based on the information provided by the resolved scales of motion. The dynamic procedure thus obviates the need for users to specify the model constant C_s in advance. The concept of the dynamic procedure is to apply a second filter (called the test filter) to the equations of motion. The new filter width Δ is equal to twice the grid filter width Δ. Both filters produce a resolved flow field. The difference between the two resolved fields is the contribution of the small scales whose size is in between the grid filter and the test filter. The information related to these scales is used to compute the model constant. The variable density formulation of the model is considered as explained below.

At the test filtered field level, the SGS stress tensor can be expressed as:

$$T_{ij} = \left(\overline{\rho u_i u_j} - \overline{\rho u_i}\,\overline{\rho u_j} / \overline{\rho} \right) \tag{13}$$

Both T_{ij} and τ_{ij} are modeled in the same way with the Smagorinsky-Lilly model, assuming scale similarity:

$$\tau_{ij} = -2C\overline{\rho}\Delta^2 |S| \left(S_{ij} - \frac{1}{3} S_{kk}\delta_{ij} \right) \tag{14}$$

$$T_{ij} = -2C\overline{\rho}\Delta^2 |S| \left(S_{ij} - \frac{1}{3} S_{kk}\delta_{ij} \right) \tag{15}$$

The coefficient C is asumed to be the same and independent of the filtering process. The grid filtered SGS and the test-filtered SGS are related by the Germano identity [17] such that:

$$L_{ij} = T_{ij} - T_{ij} = \overline{\rho} u_i u_j - \frac{1}{\overline{\rho}} \left(\overline{\rho} u_i \overline{\rho} u_j \right) \tag{16}$$

Where L_{ij} is computable from the resolved large eddy field. Substituting the grid-filter

Smagorinsky-Lilly model and Equation 15 into Equation 16, the following expressions can be derived to solve for C with the contraction obtained from the least square analysis of Lilly (1992).

$$C = \frac{\left(L_{ij} - L_{kk}\delta_{ij}/3\right)}{M_{ij}M_{ij}} \tag{17}$$

With $M_{ij} = -2\left(\Delta^2\overline{\rho}\left|S\right|S_{ij} - \Delta^2\overline{\rho}\left|S\right|S_{ij}\right)$ (18)

The obtained $C_s=\sqrt{C}$ using the dynamic Smagorinsky-Lilly model varies in time and space over a fairly wide range. To avoid numerical instability, both the numerator and the denominator in Equation 17 are locally averaged (or filtered) using the test-filter.

III MODEL DESCRIPTION

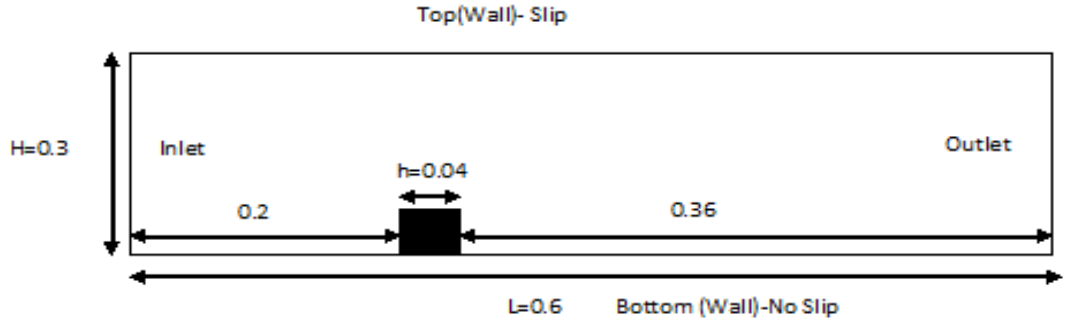

Fig. 2. 2D representation of the domain

As shown in the figure 2, the cube is taken as side is of 0.04m. The domain length is 0.6 m, the width is 0.3m and the height is also 0.3m. The cube is placed at 0.2 m away from the inlet in X direction, 0.13 m away from the left and right panel in Z direction and at zero meter i.e., at the face of the lower wall (bottom) plane in Y direction. The boundary condition is summarized below:

Table 1. Boundary Conditions

Parameters/ Domain boundary	**Bottom**	**Cube**	**Inlet**	**Outlet**	**Left**	**Right**	**Top**
P	Zero Gradient	Zero Gradient	Zero Gradient	Fixed Value (0)	Zero Gradient	Zero Gradient	Zero Gradient
U	Fixed Value (0,0,0)	Fixed Value (0,0,0)	Surface normal fixed value, Uniform (20,0,0)	Pressure Inlet-Outlet Velocity	Slip	Slip	Slip
nuSgs	Spalding wall function	Spalding wall function	Zero Gradient	Zero Gradient	Spalding wall function	Spalding wall function	Spalding wall function
k	Standard wall function	Standard wall function	Turbulent intensity inlet (0.005)	Turbulent intensity inlet (0.005)	Standard wall function	Standard wall function	Standard wall function

The inlet wind velocity is taken as (20, 0, 0) i.e. 20 m/s in horizontal direction. The domain coordinates ranges are as follows:

*A **Domain Coordinates***

Table 2. Flow domain

Coordinates	**x**	**y**	**z**
Minimum	-0.2	0	-0.13
Maximum	0.4	0.3	0.17

IV NUMERICAL APPROACH

In this numerical study OpenFoam -2.3.0 in Linux OS (Ubuntu 12.10) and Sim Flow in windows 7 (32 bit) are used to model the flow behaviour over a cube with sharp edge. It is already been established in CFD forum that Open Foam is supposed to be one of the strongest tool for CFD modelling. The transient unsteady state model was implemented by using pisoFoam which runs on PISO algorithm [19, 20]. The solution parameters are tabulated below:

Table 3. Solver and residuals

Solvers/Parameters	**Solver**	**PISO**	**Residuals**	**Relaxation**
P	GAMG		1e-04	0.3
U	PBiCG		1e-04	1
k	PBiCG		1e-04	0.8
Correctors		1		
Non orthogonal Correctors		1		

Where, GAMG-Generalised geometric-algebraic multi-grid solver

PBiCG - Preconditioned bi-conjugate gradient solver for asymmetric matrices

A. Mesh Generation

Before the description of the solvers we must first look at the meshing of the domain which is considered as the most important step to get the correct result. In the present study the meshing of the domain is done using blockMesh facility of the openFoam. The domain has been meshed by using hexahedra mesh with division 40x20x20 and with cell size of 0.015 in all the 3 direction. The cubical body has been generated in FreeCad and is exported as a .stl format in openFoam. After the importing of the cube geometry by using the snappyHexMesh utility of the openFoam the mesh of the whole geometry and the domain were refined as per the requirement. OpenFoam gives the flexibility to check the criteria for the good meshing using checkMesh utility and it is found that the mesh has been generated are acceptable as per the convention. The final mesh consists of 86912 cells and 99833 nodes. The final mesh is shown in figure 3 and the mesh of the cube is shown in figure 4. The more fine mesh could be made for the better result but because of the limitation of the computer memory the optimized mesh is being made

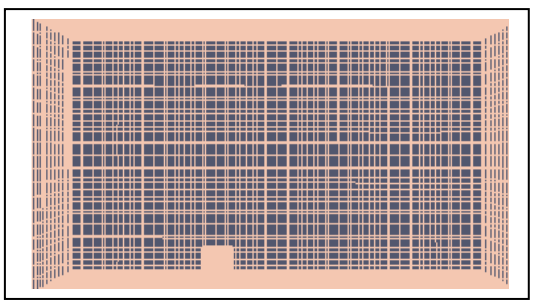

Fig.3. Final mesh of 3D Geometry

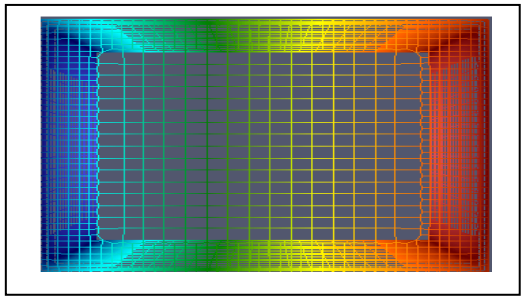

Fig.4. Top view of the meshed cube

1. PISO algorithm solver

The solver PisoFoam has run for 10000 time steps with time interval 1e-05 and after every 100 time steps the results has been written for better understandings of the run. The residual plots and the lift and drag coefficients plot have been captured during the run of the solver. The parameters of the solver is given below

Fluid: Incompressible
Type: Unsteady

Turbulence Modelling: Large eddy simulation
Model: Homogeneous Dynamic Smagorinsky
Delta: Cube root volume
Coefficient: 1
Filter: Anisotropic
Width Coefficient: 1

V. RESULTS & DISCUSSION

At the completion of the solver run for 10000 time steps we have arrived with various parameters like pressure distribution, velocity profile, yplus, vorticity etc. Before we can produce our results it is of utmost important to know whether the solver has the stability. For this purpose the best method to know is to calculate the Courant Number. As the courant number for transient flow should be less than unity for the consistency of the solver. The courant number is given by[22]

$$Co = \frac{\delta t |U|}{\delta x} \tag{19}$$

As already mentioned that the runtime is for 10000 steps and at the last iteration the maximum Courant number is noted as 0.8213591. Since the Courant number is less than unity we can say that the solver has the stability.

Let us discuss the flow parameters over the entire domain:

A. Velocity profile

The velocity profile has been generated at different points through X axis in various regions i.e. at downstream, at the cube and at the upstream to see the velocity distribution. The profiles are given below.

A.1 Velocity profile at upstream

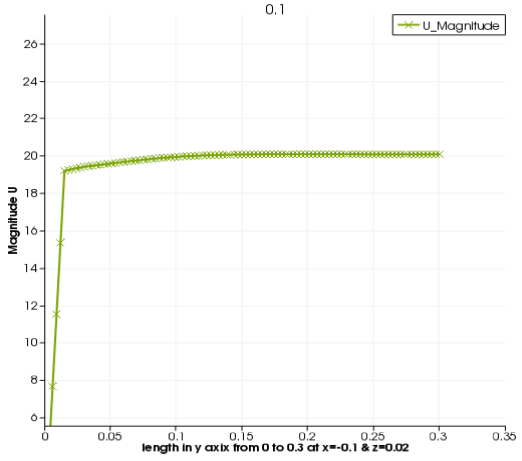

Fig.5. U magnitude at x= -0.1, z= 0.02 & through y=0 to 0.3

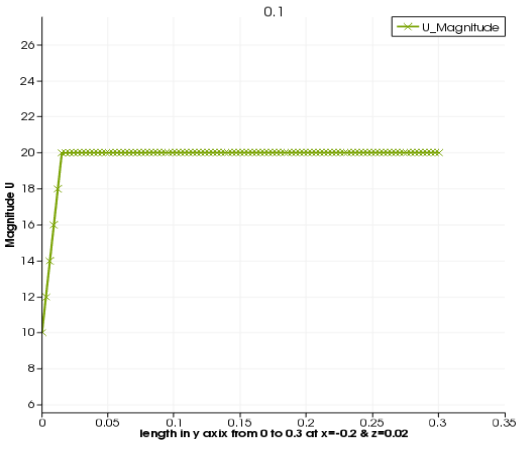

Fig.6. U magnitude at x= -0.2, z= 0.02 & through y=0 to 0.3

We have started our model with a uniform velocity of 20 m/s in the inlet of the computational domain. From figure 2. we see that the upstream section is for 0.2 which has been taken as the negative direction of x axis and the cube centre position is taken as x=0 where as the downstream section from the cube centre to the outlet is taken as positive x direction.

In the upstream section we have taken two points in figure 5. at x=-0.1 and in figure 6. at x=-0.2 which is the inlet and both at last time step 0.1. In both the plot the points are taken at the centre point in the z direction where the cube axis is lying at the centre and we move in the vertical direction from y=0 to 0.3 (i.e, through the whole height of the domain). We can see that in the later one which is at the inlet though the 0 value in the plot represents the bottom wall there is some velocity magnitude since the point is far away from the cube obstacle and as we move towards the height of the domain the velocity is constant at 20 m/s which is the inlet velocity. Where as in the first one which is closer to the cube at the wall the velocity is zero and as we move in y direction the velocity starts increasing but because of the interference of the cube it is not constant as before though it is almost 20 m/s but with slight variation.

A.2 Velocity profile at the cube position from the upper face of the cube

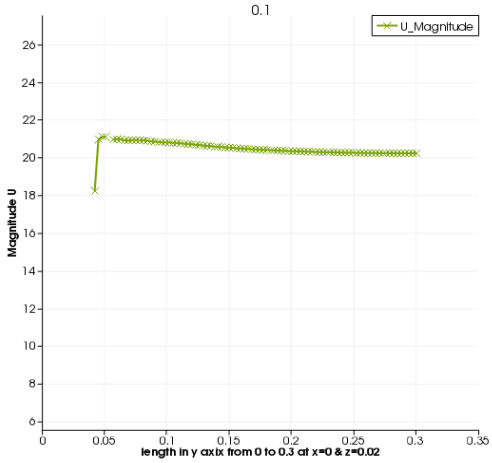

Fig.7. U magnitude at x=0, z= 0.02& through y=0 to 0.3

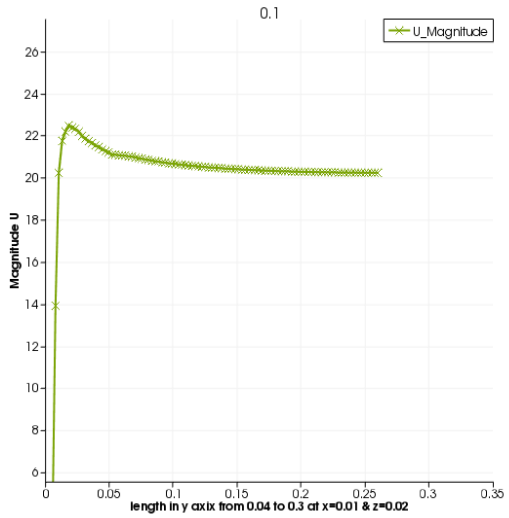

Fig.8. U magnitude at x=0.01, z= 0.02 & through y=0.04 to 0.3

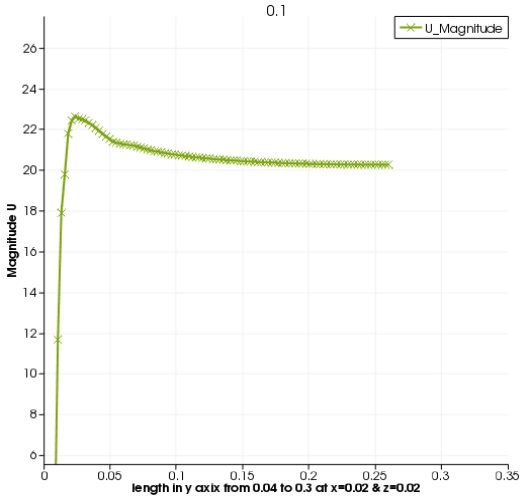

Fig.9. U magnitude at x=0.02, z= 0.02 & through y=0.04 to 0.3

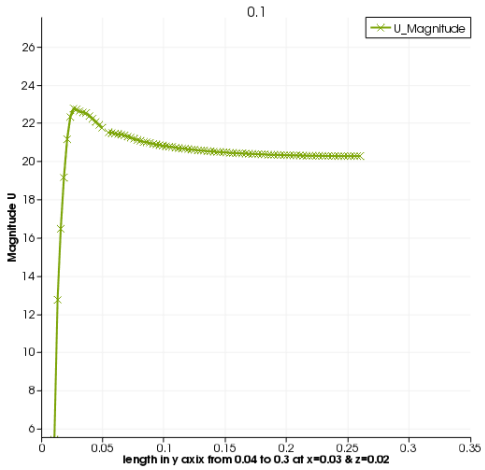

Fig.10. U magnitude at x=0.03, z= 0.02 & through y=0.04 to 0.3

The above plots from fig no. 7 to fig no 10. represent the velocity profile in the front face of the cube and the profile from the upper face of the cube to the top of the domain. As we can see the first plot is somehow aprt from the other three plots because the first plot represents the velocity distribution from the bottom of the domain touching the cube front face to the top of the domain and the other three plots start from the top of the cube. We can see that just above the cube up to a distance of nearly 0.05 the velocity goes at the maximum level and then it starts coming down and become almost at 20 m/s as we move to the top.

A.3 Velocity profile at downstream

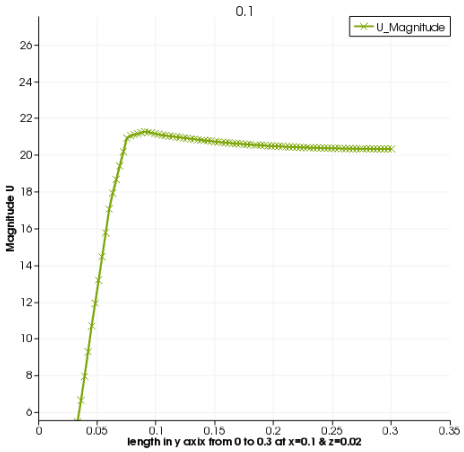

Fig.11. U magnitude at x=0.1, z= 0.02& through y=0 to 0.3

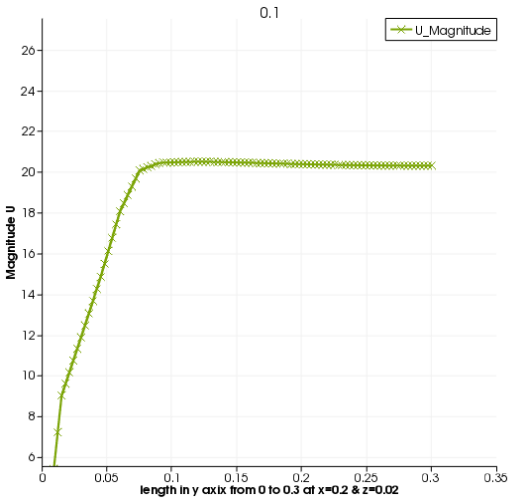

Fig.12. U magnitude at x=0.2, z= 0.02 & through y=0 to 0.3

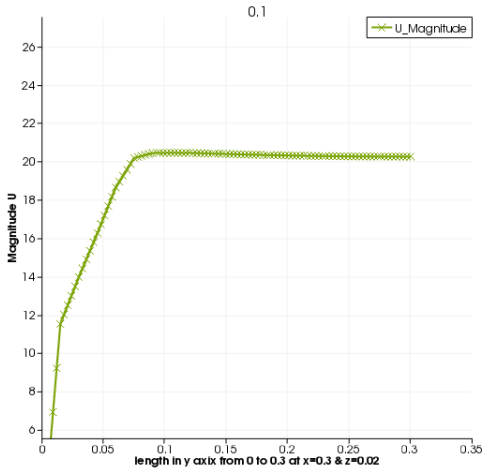

Fig.13. U magnitude at x=0.3, z= 0.02 & through y=0 to 0.3

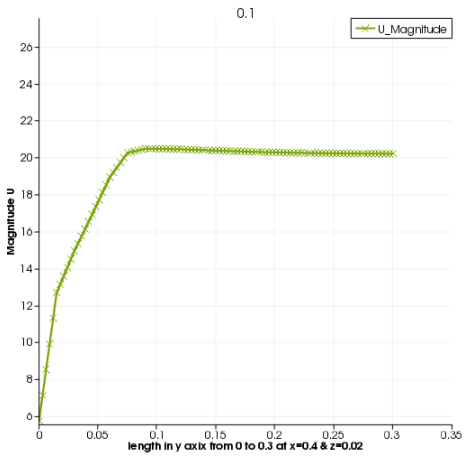

Fig.14. U magnitude at x=0.4, z= 0.02 & through y=0 to 0.3

From fig no 11 to 14 represent the velocity profile in the downstream section and form the plots it is apparent that as the distance from the cube goes on increasing in the x direction the profile are almost similar and the velocity is almost 20 m/s at the top of the domain. For the first plot since it is the nearest position respective to the cube the profile is somewhat different and because of the influence of the cube obstacles.

A.4 Dimensionless velocity profile

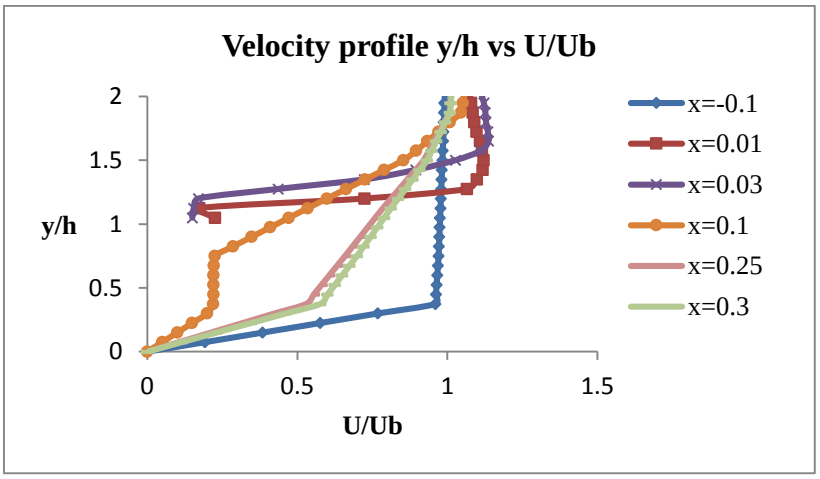

Fig 15. Plot of y/h vs U/Ub over the whole domain

It can be seen from the above plot that the blue line which corresponds the upstream position at x=-0.1 gives a undisturbed velocity profile since the obstacle has no effect

on it whereas the brown and the violet line which are on the cube top surface corresponding to x=0.01 and x=0.03 respectively gives velocity profile with lesser slopes. At the position x=0.1 ie., the yellow line which is at the downstream but very close to the exit section of the cube again gives a disturbed profile since at the downstream very close to the cube the flow is not fully developed whereas the profiles at x=0.25 and x= 0.3 ie., the red and the green lines are exactly similar with higher slopes show that the profiles are almost fully developed with low or no dependence of the obstacle.

B. Pressure Profile

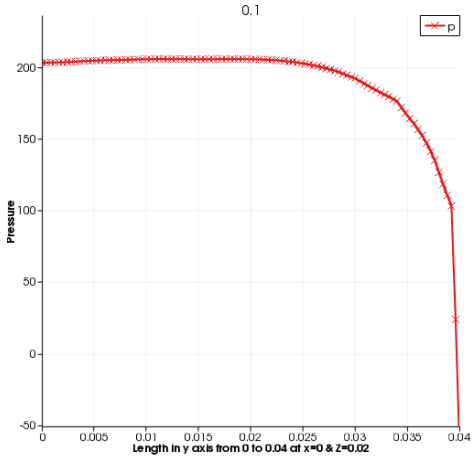

Fig 16. Pressure at the front of cube

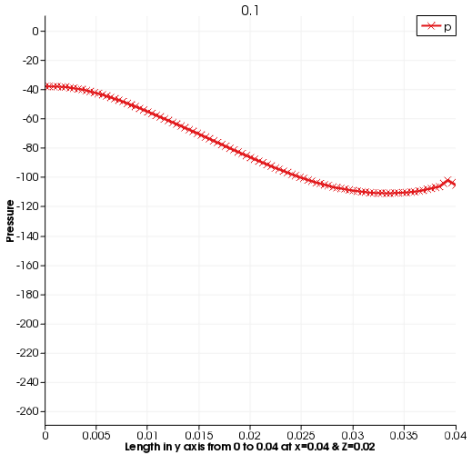

Fig 17. Pressure at the rear face of cube

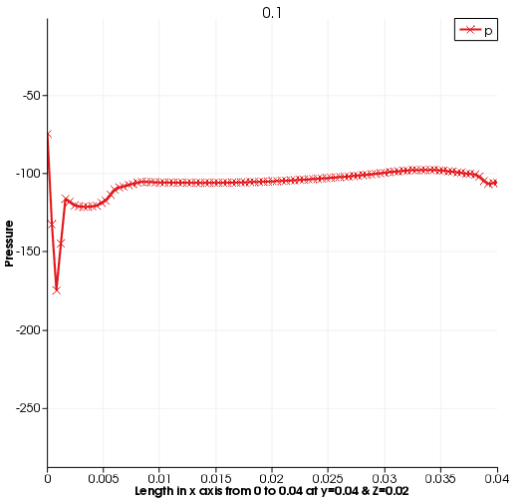

Fig 18. Pressure at the top face of cube

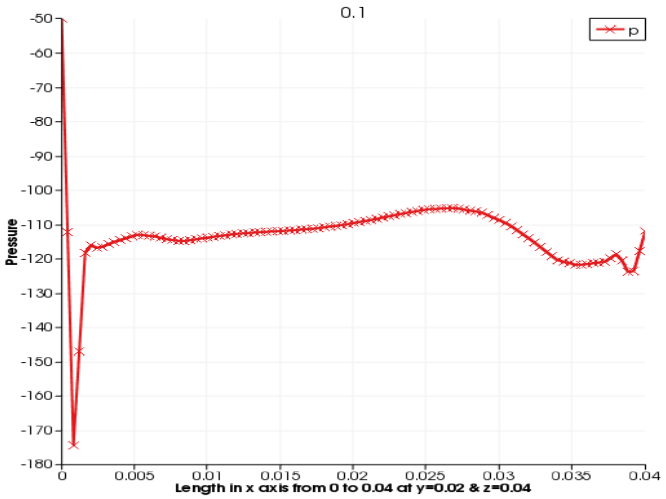

Fig 19. Pressure at the side faces of cube

From the above figures 16,17,18 & 19 we can see that at the front face only there is high pressure and the pressure is varying from 0 to 200 N/m2 and in all the four faces there are negative pressure and in all those four faces the vortex or eddies will be created and hence low pressure zone will prevail. In the front face ie., fig no. 16 the x axis is varying from 0 to 0.04 and at x=0 the pressure is maximum ie., at the bottom of the cube there is high pressure and this pressure continues almost upto $2/3^{rd}$ of the cube height and there is a sudden dip in the last $1/3^{rd}$ portion of the cube height since there is a chance of creating small eddies in the upper portion of the cube. The profile

is almost a parabolic in nature.

C. Pressure Surface plot

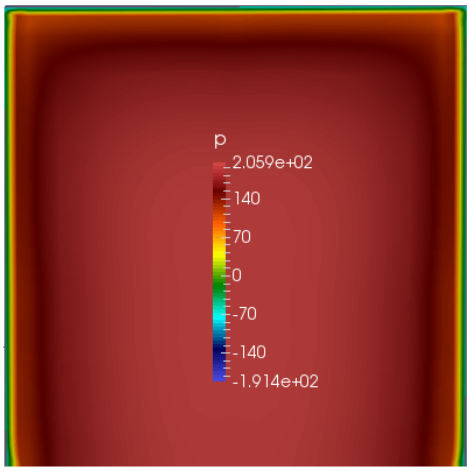

Fig 20. Surface pressure plot at the front of cube

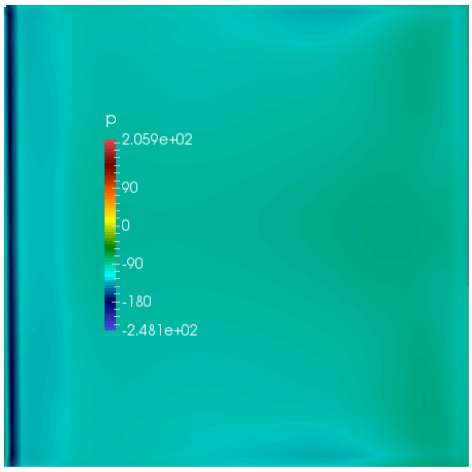

Fig 21. Surface pressure plot at the top of cube

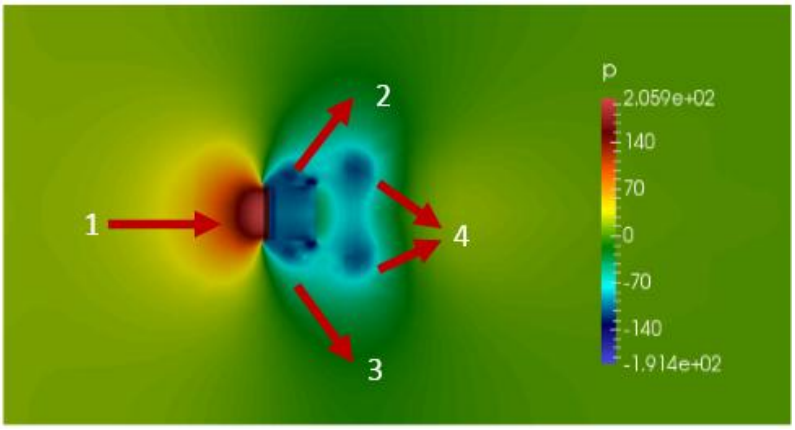

Fig 22. Surface pressure plot at X-Z bottom plane of the domain

From the above figures it can be seen that at the front face ie. the fig no 20 the pressure is very high because of the stagnation zone prevails and at the top face ie., fig no 21 the low pressure zone prevails. In the Fig no 22 it is being shown that the front face which is being marked as 1 is at high pressure while the marked no 2 & 3 show the vortex creation in the side faces and the marked no 4 indicates the creation of symmetrical vortexes in the rear face and hence low pressure zone is created.

D. Velocity Surface plot

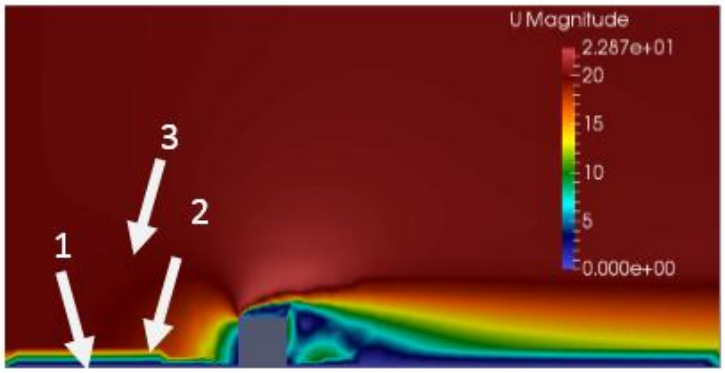

Fig 23. Velocity profile in X-Y plane

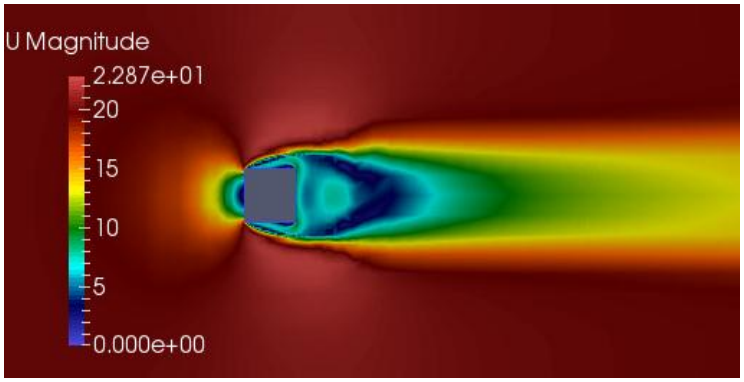

Fig 24. Velocity profile in X-Z plane

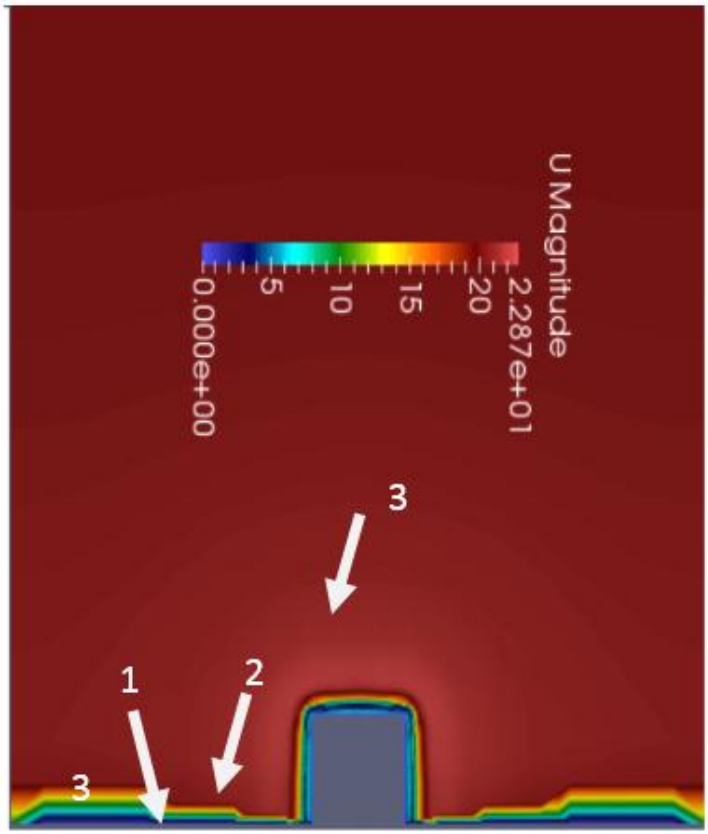

Fig 25. Velocity profile in Y-Z plane

Fig no. 23 represents the velocity surface plot in X-Y plane and it can be seen that upto 2/3rd of cube height the blue colour prevails which corresponds to zero velocity and in turn represents the stagnation zone and the pressure is very high whereas in the last 1/3rd of cube height the green and yellow colour dominates and hence there is a dip in pressure. It can be seen prominently that the boundary layer which represented

by the blue lines(1) is viscous zone, green and yellow colour lines (2) are buffer zone and the rest of the red coloured (3) are the turbulent zone and which can be validated from the well cited literatures. In the fig no 24 there is evidence of symmetrical eddies in the side faces. The fig no 25 also shows the details of boundary layer separation across the cube wall and which in turn show the structure of grid is well maintained for the study.

E. Pressure contour

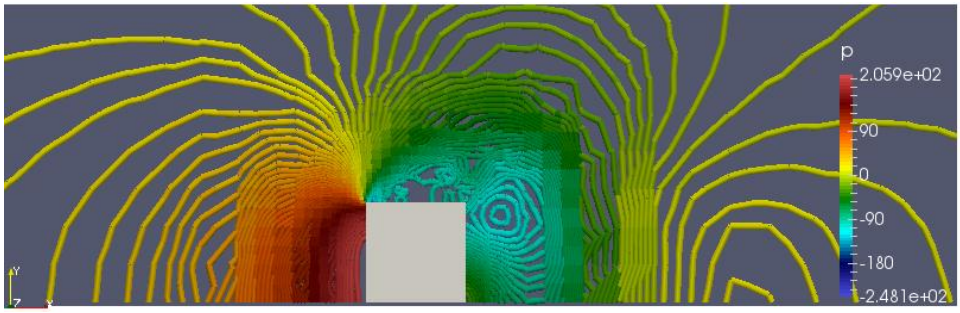

Fig 26. Pressure contour plot coloured by pressure in X-Y plane

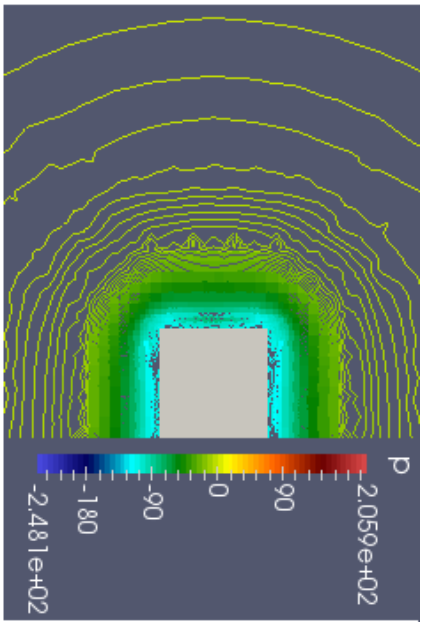

Fig 26. Pressure contour plot coloured by pressure in Y-Z plane

Fig no. 25 shows that at the top of the cube prominent vortex generation and the

layers are getting widen to give uniform pressure profile away from the cube face where as in the rear portion we see the vortex like horse shoe. Fig no 26 it can be visualise that at the top and at the sides of the cube the low pressure zones are prominent.

F. Streamline plot

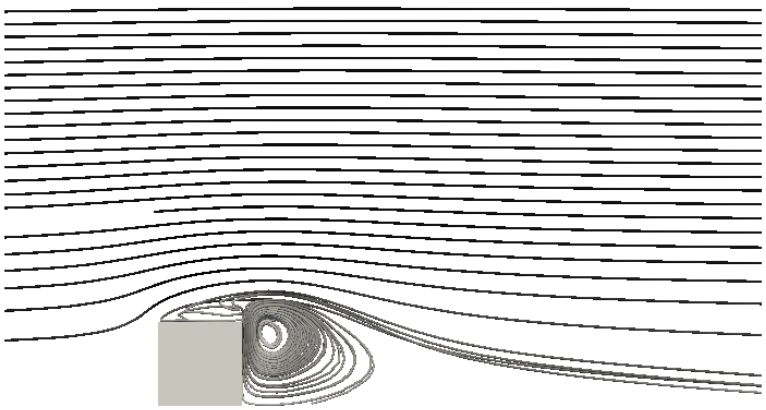

Fig 27. Streamline at time 0.07

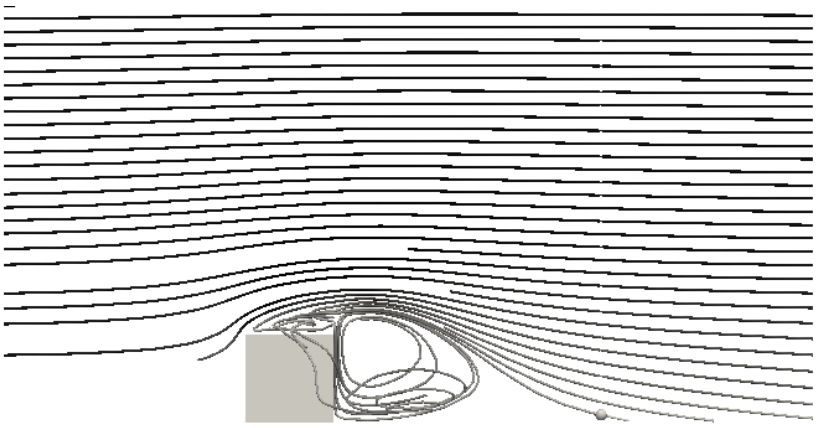

Fig 28. Streamline at time 0.1

In both the above plots fig no. 27 & 28 we can see that there are vortex at the top and at the rear face of the cube and hence the pressure are low at those zones. Here it can be seen that the reattachment is almost 3h distance away from the cube.

G. Vorticity

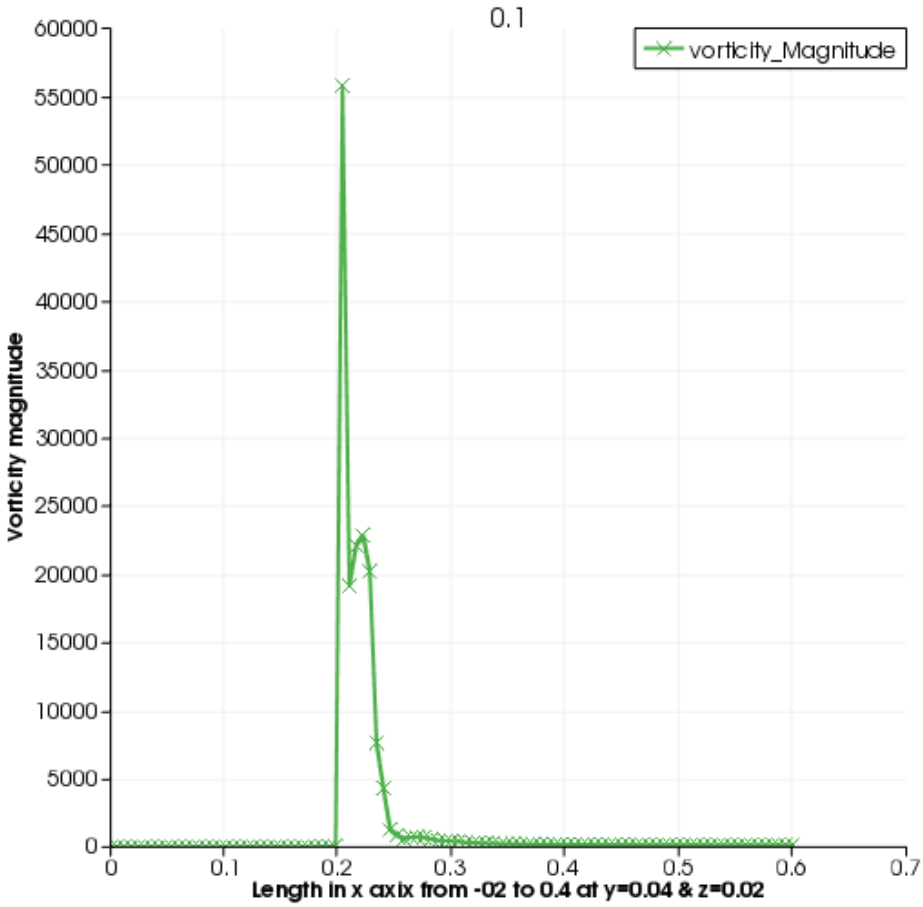

Fig 29. Vorticity magnitude at the rear face at time 0.1

The above fig shows the vorticity is very high just adjacent to the rear face of the cube and as we move far from the cube the vorticity diminishes and subsequently the velocity profile becomes uniform which can be verify from the velocity profile plot fig no 15.

H. y plus

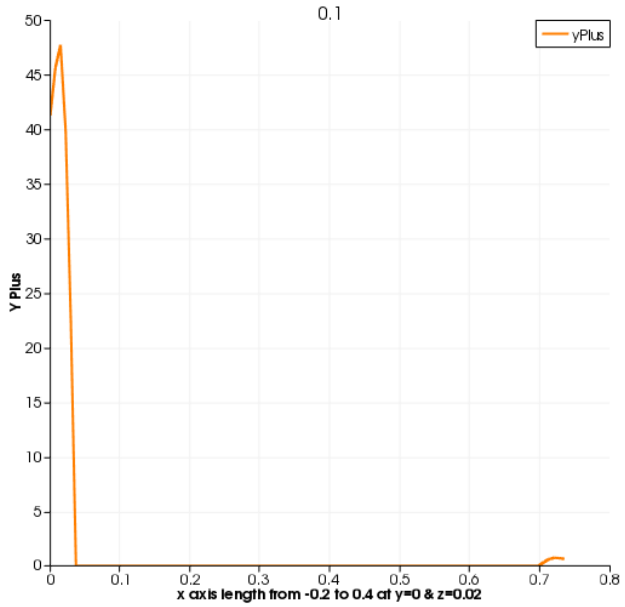

Fig 30. Plot of y plus through x axis at the bottom of the domain

The plot shows that the y plus at the bottom of the domain is very close to zero and we know from literature that the y plus value in the viscous zone is 0<yplus<5 and since the bottom is taken as wall so the viscous zone will reside very close to wall which can further be verified from the fig no. 23. As it can be seen that very close to the inlet the y plus is high this is because at the inlet turbulent boundary condition is imposed and in the turbulent zone the range of y plus>30. This implies that the grid resolution for the above study is up to the acceptable limit.

I. Residuals Plot

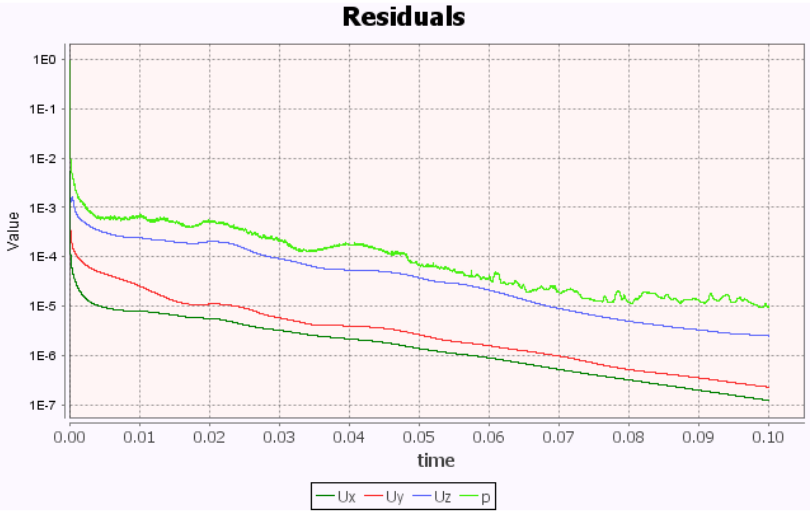

Fig 31. Residuals plot

The above plot shows the residuals and as the table no 3 gives the specification of residuals it matches with the plot after the simulation time which shows the fulfilling criteria of the solver.

J. Force Coefficients

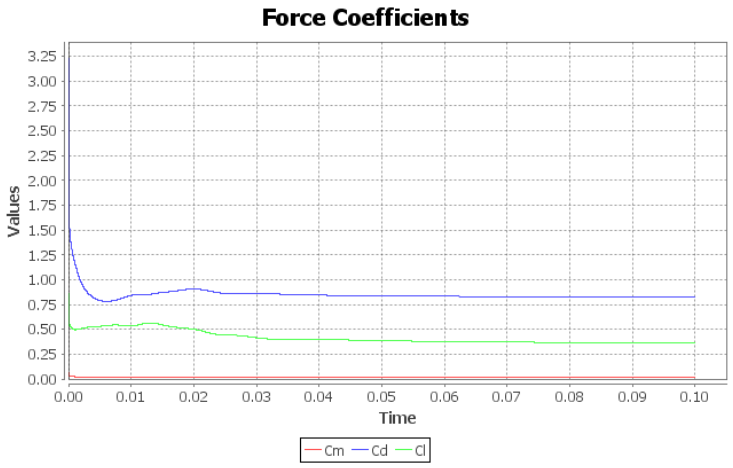

Fig 32. Force Coefficients

It can be seen from the above plot that the drag coefficient is almost 0.8 (in between 0.75 and 1) and the lift coefficient is 0.375. In the cubical model the drag force will always dominate the lift force which is exactly the same in the case. generally for cube the drag force comes nearly 0.8 [21] which is same as in our case. We know the drag coefficient C_D is a long time mean value of normalised drag force. We seek an approximate drag coefficient C_D over a finite time interval [0,0.1].In case of validation of the solver and the result achieved, we choose to verify the Strouhal Number which is one of the benchmark. Strouhal No can be described as:

$$S_t = (f\ D/U) \tag{20}$$

Where f= Frequency for vortex Shedding, D= Diameter or the length scale, U=Bulk fluid velocity.

Alexander Yakhot et. al.(2006) [23] have worked on the dominant characteristic frequency in the rear wake and obtained Strouhal number St = fh/Ub = 0.104 (based on the cube height h and the bulk velocity Ub) using FFT analysis of the power spectral density (PSD) of the computed spanwise velocity which was consistent with the experimental Strouhal numbers of 0.095 and 0.109 reported in Meinders et al. (1999) [5] and Meinders and Hanjalic (1999) [25], respectively.

To find vortex shedding frequency, the Fast Fourier Transformation of the time domain data of lift coefficient is used in Matlab and the fft plot is given below:

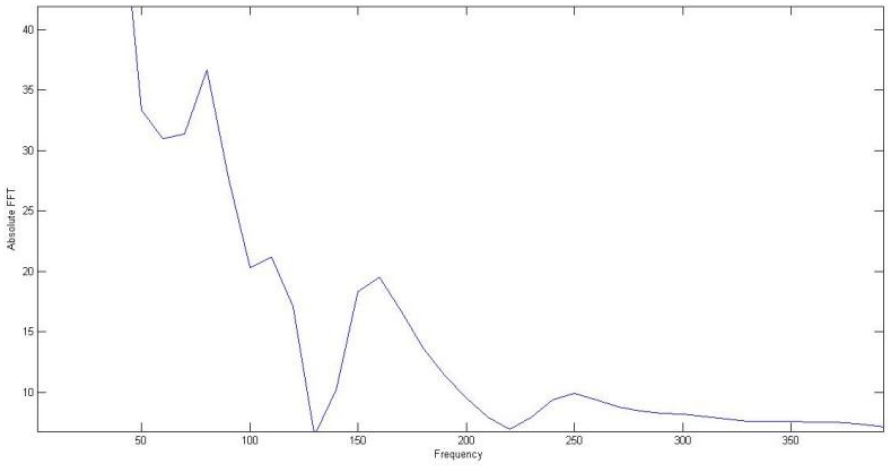

Fig 33. Fast Fourier Transformation (FFT) of lift force

From the above figure it can be observed that the highet peak of the FFT is almost at frequency 50 and if we take f=50 in the formula of Strouhal no it comes as S_t= (f h/U) =(50*0.04)/20=0.1 which comes in agreement with the other published work discussed in literature earlier. Thorsten Stoesser et. al. have worked on "les of flow over multiple cubes" and they have published their result on 2003[25] and they have reported the Strouhal no of 0.11 for Reynolds no 13000 which also very close to our result. From literature as a general concept the strouhal number for flow over a cube should be less than 0.2.

K. Drag force prediction using neural network

The time series data of drag force has been taken for analysis in the MATLAB neural network. we have total 10000 samples of drag coefficients in the time interval [0,0.1]. The code has been written in MATLAB to implement NARNET architecture and close loop analysis. 5000 samples has been taken for training out of 10000 with 3 hidden neuron and the predicted error is almost 0.1 which is quite acceptable. The error plot is given below:

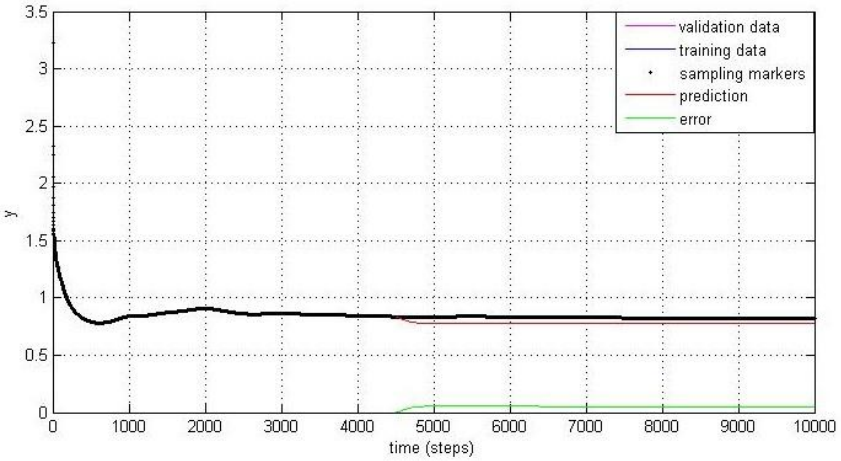

Fig.34. Neural network drag prediction& error validation

From the plot it can been seen that the drag prediction is quite accurate for the working Reynolds number of 80,000 and hence neural network can be another tool to predict the drag coefficient accurately.

VI CONCLUSIONS

Large eddy simulation was performed using Smagorinsky for flow over a wall mounted cube using PISO algorithm for Reynolds number of 80000. Fully developed flow was considered in the inlet. Various results like velocity distribution, velocity profile, pressure distribution over the front, top and rear face of the cube were found along with the force coefficients. We have also shown the variation of y plus in the bottom wall of the flow domain. Some interesting characteristic regarding the flow field were observed like the initial drag coefficient is very high and as the time progresses the drag coefficient tries to reach a steady state value. Strouhal number was found by finding the maximum frequency for vortex shedding for Karman Vortex Street and found that the Strouhal no is with accordance with other published results. We also have shown that the horse-shoe type vortex in the adjacent rear face of the cube. Overall we can conclude that the Large eddy simulation can describe the flow phenomena in turbulence field with good resolution and can be a suitable alternative to direct numerical simulation (DNS) which is time consuming and also costly at the same time. The neural network is used to validate the drag coefficients obtained by the simulation and was found acceptable as all the predicted value are within the acceptable error range.

REFERENCES

[1] Mohd. Ariff, Salim M. Salim and Siew Cheong Cheah, " Wall y^+ approach for dealing with turbulent flow over a surface mounted cube : Part – I – Low Reynolds no." Seventh International conference on CFD in the minerals & process Industries, CSIRO, Melbourne, Australia, 9-11 Dec. 2009.

[2] Kolmogorov A. N. The local structure of turbulence in incompressible viscous fluid for very large Reynolds numbers.Dokl. Akad. Nauk., Vol. 30, pp. 301 – 305, 1941. Reprinted Proc. Royal Soc. London; 434; 9; 1991.

[3] Martinuzzi, R., Tropea, C., 1993. The flow around surface-mounted, prismatic obstacles placed in a fully developed channel flow. J Fluid Eng. 115(1), 85-91.

[4] Hussein, H.J., Martinuzzi, R.J., 1996.Energy balance for turbulent flow around a surface-mounted cube placed in a channel. Phys. Fluids 8(3), 764-780.

[5] Meinders, E.R., Hanjalic, K., Martinuzzi, R.J., 1999. Experimental study of the local convection heat transfer from a wall-mounted cube in turbulent channel flow. Trans. ASME J. Heat Transfer, 121, 564-573.

[6] Iaccarino, G., Ooi, A., Durbin, P.A., Behnia, M. 2003. Reynolds averaged simulation of unsteady separated flow. Int. J. Heat Fluid Flow 24, 147-156.

[7] Lakehal, D., Rodi, W., 1997. Calculation of the flow past a surface-mounted cube with two-layer turbulence models. J. Wind Eng. Ind. Aero-dyn. 67 and 68, 65-78.

[8] Krajnovic, S., Davidson, L., 1999. Large-eddy simulation of the flow around a surface-mounted cube using a dynamic one-equation sub grid model. In: The First Int. Symp. On turbulence and Shear Flow Phenomena, Eds,: S. Banerjee and J. Eaton, Beggel House, Inc., New York.

[9] Krajnovic, S., Davidson, L., 2001. Large-eddy simulation of the flow around a three-dimensional bluff body. AIAA 2001-0432, 39th AIAA Aerospace sciences meeting and Exhibit, January 8-11, Reno, Nevada.

[10] Niceno, B., Dronkers, A.D. T., Hanjalic, K., 2002. Turbulent heat transfer from a multi-layered wall-mounted cube matrix: a large eddy simulation, Int. J. Heat Fluid Flow 23, 173-185.

[11] Rodi, W., Ferziger, J., Breuer, M., Pourquie, M., 1997. Status of large-eddy simulation: results of a workshop, J. Fluids Engg. 119, 248-262.

[12] Shah, K.B., Ferziger, J.H., 1997, A fluid mechanician's view of wind engineering: Large eddy simulation of flow past a cubic obstacle. J. wind Engg. Ind. Aerodyn. 67and 68, 211-224.

[13] Alexander Yakhot , Heping Liu a, Nikolay Nikitin , Turbulent flow around a wall-mounted cube: A direct numerical simulation, International Journal of Heat and Fluid Flow 27 (2006) 994–1009

[14] J. O.Hinze. Turbulence. McGraw-Hill Publishing Co., New York, 1975.

[15] G. Erlebacher, M. Y. Hussaini, C. G. Speziale, and T. A. Zang. Toward the Large-Eddy Simulation of Compressible Turbulent Flows. J. Fluid Mech.,

238:155-185, 1992.

[16] J. Smagorinsky, General Circulation Experiments with the Primitive Equations. I. The Basic Experiment. Month. Wea. Rev., 91:99-164, 1963.

[17] M. Germano, U. Piomelli, P. Moin, and W. H. Cabot. Dynamic Subgrid-Scale Eddy Viscosity Model. In Summer Workshop, Center for Turbulence Research, Stanford, CA, 1996.

[18] D. K. Lilly, A Proposed Modification of the Germano Subgrid-Scale Closure Model. Physics of Fluids, 4:633-635, 1992.

[19] Issa R.I., Solution of the implicitly discretised fluid flow equations by operator-splitting, Journal of Computational Physics (ISSN 0021-9991), vol. 62, p. 40-65. Jan. 1986, p. 40-65.

[20] Versteeg H K & Malalasekera W, An Introduction to Computational Fluid Dynamics, The Finite Volume Method: Longman Scientific & Technical, pp. 150-154, (1995).

[21] http://www.engineeringtoolbox.com/drag-coefficient-d_627.html

[22] OpenFoam website: www.openfoam.org/ docs/user/cavity.php#x5-120002.1.3

[23] Alexander Yakhot, Heping Liu, Nikolay Nikitin , Turbulent flow around a wall-mounted cube: A direct numerical simulation, International Journal of Heat and Fluid Flow 27 (2006) 994–1009

[24] Meinders, E., Hanjalic´, Vortex structure and heat transfer in turbulent flow over a wall-mounted matrix of cubes. Int. J. Heat Fluid Flow 20, 255–267, 1999.

[25] Thorsten Stoesser , Fabrice Mathey , Jochen Fröhlich 3, Wolfgang Rodi, “Les Of Flow Over Multiple Cubes” ERCOFTAC Bulletin, March 2003

AUTHOR PROFILE

Bibhab Kumar Lodh

Bibhab Kumar Lodh has acquired his B.tech degree in Chemical Engineering with first class with distinction from Shivaji University Kolhapur in 1999 and M.Tech Degree from IIT BHU (formerly I.T. BHU) in 2001 with 8.55 CGPA. He has almost nine years of industrial Experience and five years of teaching experience. He is presently engaged in Assistant Professor in the Department of Chemical Engineering at NIT Agartala and pursuing his PhD in the arena of CFD at NIT Agartala.

Ajoy Kumar Das

Ajoy Kumar Das has acquired his B.E degree in Mechanical Engineering from NIT Surathkal in 1994, M.Tech Degree from IIT Madras in 1996 and PhD degree from IIT Kharagpur in the year 2010. He has vast teaching experience and presently he is engaged as as Associate Professor in the Department of Mechanical Engineering at NIT Agartala and also working as Dean Academic at NIT Agartala.

N. Singh

N. Singh has acquired his PhD Degree from IIT Kharagpur and joined the IIT Kharagpur in the year 1984. He has vast experience in teaching and research in the arena of Aerospace engineering. He is presently working as a professor in the Department of Aerospace Engineering at IIT Kharagpur.